Superhalogen Properties of Fluorinated Coinage Metal Clusters†

ARTICLE *in* THE JOURNAL OF PHYSICAL CHEMISTRY C · JULY 2010

Impact Factor: 4.77 · DOI: 10.1021/jp101807s

Superhalogen Properties of Fluorinated Coinage Metal Clusters†

Pratik Koirala,‡ Mary Willis,§ Boggavarapu Kiran,|| Anil K. Kandalam,‡,* and Puru Jena*,§

Department of Physics, Department of Chemistry, McNeese State University, Lake Charles, Louisiana 70609 and Department of Physics, Virginia Commonwealth University, Richmond, Virginia 23284

Received: February 28, 2010; Revised Manuscript Received: June 1, 2010

Equilibrium geometries and ground state spin multiplicities of neutral and anionic coinage metal fluoride XF_n clusters (X = Cu, Ag, and Au; $n = 1-7$) are obtained from density functional theory-based calculations. Our results show that in the case of neutral and anionic CuF_n and AgF_n clusters, a maximum of 4 F atoms ($n_{max} = 4$) can be bound atomically to the metal atoms, while remaining F atoms bind to the other F atoms to form F_2 units. In contrast, a Au atom can bind up to six F atoms dissociatively. This contrasting binding scenario observed for these metal fluoride clusters is explained using the natural bond orbital analysis. The neutral XF_n (X = Cu, Ag) clusters are stable against dissociation into X and F atoms up to $n = 6$, while AuF_n clusters are stable up to $n = 7$. Similarly, with the exception of AgF_7 and AuF_6, all neutral clusters studied are stable against dissociation into F_2 molecules. On the other hand, XF_n^- clusters are stable against dissociation into F atoms and F_2 molecules over the entire size range, indicating the increased stability of anionic species over their neutral counterparts. Even more striking is the fact that the electron affinities of these clusters can be as large as 8 eV, far exceeding the electron affinity of Cl that has the highest value in the periodic table. These clusters are thus classified as superhalogens.

I. Introduction

Driven by finite size, low-dimension, reduced coordination, and large surface to volume ratio, materials at the nanoscale possess uncommon properties seldom seen in the bulk phase. A fundamental insight into how these parameters influence the structure−property relationships can be achieved through studies of atomic clusters where their size and composition can be controlled one atom at a time. While early works on clusters were aimed at understanding how properties of matter evolve from atoms to bulk, discoveries of many novel properties of clusters over the last three decades has given rise to the hope that clusters can be used as building blocks of materials. One of these properties is the superatom behavior of clusters. It was realized that the size and composition of a cluster can be tailored in such a way that it can mimic the property of an atom in the periodic table. These clusters can then be used as building blocks of a new class of materials called cluster-assembled materials. The idea of clusters as superatoms arose with the discovery by Knight and co-workers[1] that Na clusters consisting of 8, 20, 40, and so forth, atoms are very stable and their stability arose from electronic shell closures much as those of magic nuclei whose stability are attributed to the nuclear shell closure rule. Later experiments by Castleman and co-workers[2] on Al_{13}^- showed that clusters with closed electronic shells are also chemically more inert than their neighbors. Khanna and Jena[3] used these results to develop the concept of a superatom that can be created by combining both geometric and electronic shell closure rules. The first example in this series was the Al_{13} cluster. With one electron less than what is needed to fill electronic shells, Al_{13} behaves as a halogen atom and has an electron affinity that is almost identical with that of Cl. Thus, it was proposed[3] that a new class of salts can be synthesized by using clusters such as Al_{13} as a building block. Later experiments[4] have proved this to be true and KAl_{13} was found to possess the properties of a salt.

Another concept of clusters that was also developed during this period is that of superhalogens. It was found that a cluster consisting of a metal atom at the center and surrounded by several oxygen or halogen atoms can have electron affinities that are larger than that of Cl, the element with the highest electron affinity in the periodic table. Clusters exhibiting such large electron affinities are termed superhalogens. The large EA values are due to the extra electron's delocalization over the electronegative oxygen or halogen atoms. Gutsev and Boldyrev[5] proposed that a cluster with composition $MX_{(n+1)/m}$ can be a superhalogen where M is the central metal atom and X is the electronegative atom, with n being the maximal formal valence of M, and m is the valence of the X. Gutsev et al.[6] later extended this idea to transition metal atoms and showed that MnO_4 can be a superhalogen since the maximum valency of Mn is 7. Indeed its predicted electron affinity of 5 eV was confirmed by experiments.[6] $KMnO_4$ is a well-known oxidizing agent. Other 3d-transition metal oxide clusters, such as FeO_4 and CrO_4, have also been predicted to behave as superhalogens.[7]

Salts containing F have been a subject of great interest for the past several decades and reaction of gold and platinum metals (except rhodium) with F_2 have yielded salts of MF_6^- (M = Ru, Os, Ir, Pt, Au).[8−10] Gold hexafluoride is the most powerful oxidizing hexafluoride of the third transition series and $LiAuF_6$ salt has been synthesized.[10] The electron affinity of AuF_6 has been estimated as 10 ± 0.5 eV.[11] Gold heptafluoride was synthesized[12] by reacting AuF_5 with atomic fluorine more than 20 years ago and the fact that Au can exist in an oxidation state +7 initially met with skepticism.[13] Recent theoretical calculations[14] have shown that AuF_7 is indeed a stable structure (a minimum), albeit it exists as $(AuF_5)F_2$ complex. However,

† Part of the special issue "Protected Metallic Clusters, Quantum Wells and Metallic Nanocrystal Molecules".

* To whom correspondence should be addressed. Email: akandalam@mcneese.edu (A. K.); jena@vcu.edu (P. J.).

‡ Department of Physics, McNeese State University.

§ Department of Physics, Virginia Commonwealth University.

|| Department of Chemistry, McNeese State University.

10.1021/jp101807s
Published on Web 07/21/2010

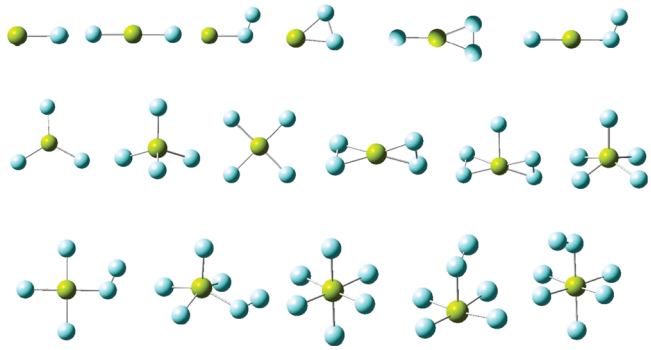

Figure 1. Various structural configurations considered for the optimization of the geometries of XF_n ($n = 1-7$) clusters. Blue and yellow correspond to F and coinage metal atoms, respectively.

Ag, which is also a coinage metal, does not show an oxidation state as high as that of gold and its highest oxidation state has been found to be +3.[10] Copper, on the other hand, is known to exhibit an oxidation state of +1 and +2 exemplified by Cu_2O and CuO. Recent work, however, has found the oxidation state of Cu to be +3.[10] The reasons why different coinage metal atoms exhibit different oxidation states has not been systematically investigated. In a recent work, Wang et al.[15] have studied the interaction of a Cu atom with up to six F atoms and reported that all these CuF_n clusters have positive frequencies and hence correspond to minima on the potential energy surface. It was reported that the neutral CuF_n clusters were stable against fragmentation into F and F_2 for $n \leq 4$, while their anionic counterparts were reported to be stable against fragmentation into F and F_2 up to $n = 5$. More importantly, the electron affinities of these clusters steadily rise reaching a peak value of 7.2 eV for CuF_5.

No systematic study of the structure and electronic properties of AgF_n and AuF_n clusters as a function of n is available. The possibility of synthesizing salts with varying F content and the use of F-containing salts in combating biological agents make a systematic understanding of the interaction of F atoms with metal atoms important. With this motivation, we present here a systematic study of the structure, stability, and electron affinities of AgF_n and AuF_n clusters up to $n = 7$. To compare the similarities and differences in the structural and electronic properties of all of the coinage fluoride XF_n (X = Cu, Ag, and Au) clusters at the same level of theory, we have also carried out the calculations for neutral and anionic CuF_n clusters.

II. Computational Procedure

The calculations were carried out under the framework of density functional theory using Gausian03 software.[16] B3LYP functional form[17,18] for the gradient corrected exchange and correlation potentials was employed, while the SDD basis set, which includes relativistic effects, was used for Cu, Ag, and Au atoms and the 6-311+G* basis for F. In the SDD basis set, the number of core electrons replaced by the ECP for Cu, Ag, and Au are 10, 28, and 60 respectively. To obtain the lowest energy structure of XF_n clusters (X = Ag and Au, $n = 1-7$), we considered several initial structures where F atoms are bound both atomically and molecularly. These geometries are given in Figure 1. For each of these geometries calculations were carried out for the two lowest spin states (singlet and triplet for even electron systems and doublet and quartet for the odd electron systems). We have optimized the geometries of both neutral and anionic clusters without any symmetry constraint for two lowest spin states. The convergence in total energy and gradient was set to 10^{-9} hartree and 10^{-4} hartree/Å, respectively. Vibrational frequency calculations were also carried out to confirm the stability of these isomers. The accuracy of this method as well as those of basis sets and exchange correlation functional is well established.[19]

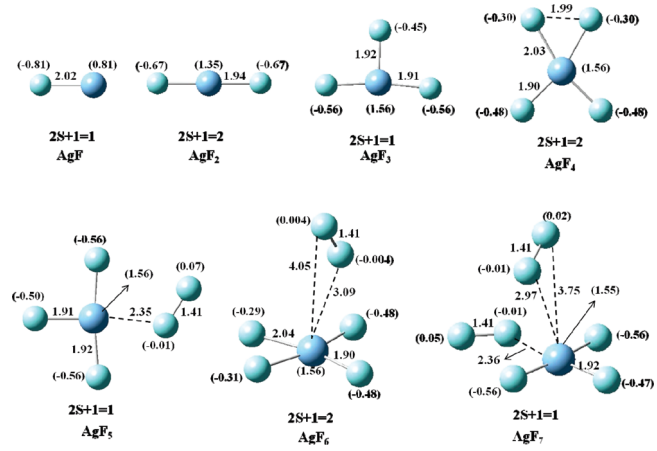

Figure 2. Equilibrium geometries of neutral AgF_n ($n = 1-7$) clusters along with their preferred spin multiplicities. The numbers in the parentheses are the NPA charges. All the bond lengths are given in Å.

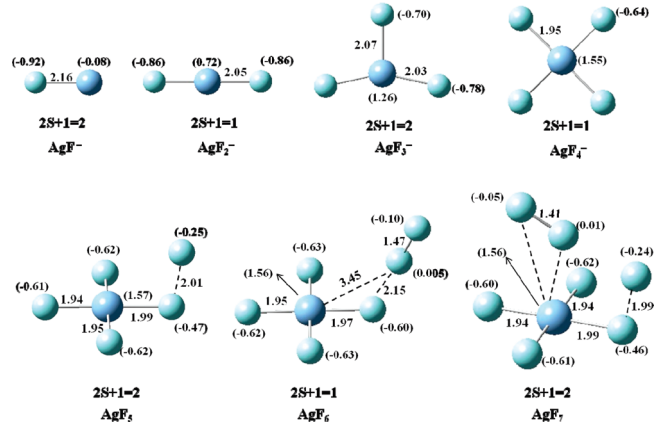

Figure 3. Equilibrium geometries of negatively charged AgF_n ($n = 1-7$) clusters along with their preferred spin multiplicities. The numbers in the parentheses are the NPA charges. All the bond lengths are given in Å.

III. Results and Discussions

A. AgF_n Clusters. We begin our discussion with the equilibrium geometries of AgF_n clusters. The lowest energy isomers and the spin multiplicities of neutral and anionic AgF_n clusters are shown in Figures 2 and 3, respectively. The natural population analysis (NPA) charges on each atom in the cluster, calculated using NBO (natural bond orbital) method, are also shown. We can divide the structures of neutral and anionic AgF_n clusters into two categories, (i) AgF_n ($n = 1-4$), where all of the F atoms bind atomically to the Ag atom, (ii) AgF_n ($n = 5-7$), where either F_2 molecule binds to the AgF_{n-2} or an F atom is weakly bound to AgF_{n-1}, thus forming $(AgF_{n-2})F_2$ or $(AgF_{n-1})F$ complexes. For example, in the case of neutral AgF_5, one of the F atoms bind to another F atom instead of to the Ag atom, thus neutral AgF_5 can be considered as $(AgF_3)F_2$ cluster, while in its anionic counterpart, the F atom is weakly bound to an F atom of the AgF_4^- cluster. This trend becomes more evident in AgF_6 (AgF_6^-) where a F_2 molecule binds weakly to the AgF_4 (AgF_4^-) moiety. In the case of AgF_7 (AgF_7^-), one

TABLE 1: Dissociation Energies of Neutral and Anionic AgF_n Clusters ($n = 1-7$) Given in Equations 1−5 of the Text[a]

cluster	$\Delta E^{neutral}$	ΔE_n^{anion} (1)	ΔE_n^{anion} (2)	$\Delta \varepsilon_n^{neutral}$	$\Delta \varepsilon_n^{anion}$
AgF	3.20	3.56	1.45		
AgF_2	1.85	5.01	3.26	3.81	7.19
AgF_3	1.16	1.96	3.23	1.77	5.58
AgF_4	0.98	2.54	4.61	0.77	3.12
AgF_5	0.60	0.50	4.13	0.21	1.67
AgF_6	0.82	1.05	4.57	0.05	0.17
AgF_7	0.62	0.41	4.17	0.11	0.08

[a] All energies are given in eV.

can clearly observe that only 3(4) F atoms bind to the central metal atom, while the rest of the F atoms form F_2 and interact with the AgF_3 (AgF_4^-) units. The structural transformation, from isomers containing atomic F to isomers with F_2 molecules, at AgF_5 reveals that the oxidation state of Ag in neutral species can go as high as +4, while in the case of anionic clusters, the maximum oxidation state of Ag is +3. It is to be noted here that the highest oxidation state of Ag was earlier reported[20] to be +3, in AgF_4^-. The average bond distance between Ag and F in neutral AgF_n ($n \leq 3$) clusters is smaller than that of their corresponding anions as is usually the case. However, as the number of F atoms increase, the Ag−F bond lengths in anionic clusters become smaller than those in the neutral clusters, indicating the increasing stability of the anions with the size of the cluster. We will show in the following that this trend reflects large electron affinities of AgF_n clusters.

The thermodynamic stabilities of the neutral AgF_n clusters against dissociation into AgF_{n-1} + F are calculated from the following equation

$$\Delta E_n^{neutral} = -[E(AgF_n) - E(AgF_{n-1}) - E(F)] \quad (1)$$

For the anion there are two dissociation paths; one where the cluster fragments into AgF_{n-1}^- + F and the other where it fragments into AgF_{n-1} + F^-. The corresponding dissociation energies are calculated as follows

$$\Delta E_n^{anion}(1) = -[E(AgF_n^-) - E(AgF_{n-1}^-) - E(F)] \quad (2)$$

$$\Delta E_n^{anion}(2) = -[E(AgF_n^-) - E(AgF_{n-1}) - E(F^-)] \quad (3)$$

In Table 1 we list these values. Note that neutral AgF_n clusters are stable up to $n = 6$. In the case of the anion cluster the preferred fragmentation pathway is the one for which ΔE_n^{anion} is the lowest. Thus for $n = 1$ and 2, the negative charge resides on the F atom during the dissociation, while for larger clusters, AgF_{n-1} fragment carries the extra charge. Most strikingly, in the case of AgF_5^-, the dissociation into AgF_4^- + F as opposed to AgF_4 + F^- fragments is favored by 3.63 eV (see Table 1), reflecting the fact that in AgF_5^- the negative charge resides on AgF_4 part of the cluster. The low energy cost (0.50 eV) to dissociate AgF_5^- into AgF_4^- and F, combined with the NPA charges on the atoms (see Figure 3), further confirm this conclusion. Therefore, AgF_5^- is actually (AgF_4^-)F complex. All the anionic clusters are stable against dissociation. The energetics associated with dissociation into a F_2 molecule are calculated using equations

$$\Delta \varepsilon_n^{neutral} = [E(AgF_n) - E(AgF_{n-2}) - E(F_2)] \quad (4)$$

$$\Delta \varepsilon_n^{anion} = [E(AgF_n^-) - E(AgF_{n-2}^-) - E(F_2)] \quad (5)$$

The results are also given in Table 1. Here we note that neutral and anionic AgF_n clusters are stable against dissociation into F_2 up to $n = 6$. In the case of neutral AgF_5 and AgF_6, dissociation into and AgF_{n-2} and F_2 is more favorable than dissociation into AgF_{n-1} and F. In fact, in the case of AgF_6, the F_2 is very weakly bound to the AgF_4 with binding energy of 0.05 eV. This is again consistent with the fact that beyond AgF_4, the AgF_n species form complexes containing F_2 molecules. Similarly, in anionic AgF_6 and AgF_7 species, the dissociation into AgF_{n-2}^- and F_2 is more favorable. In AgF_6^-, F_2 binds weakly to the AgF_4^- with a binding energy of 0.17 eV. The dissociation energies in conjunction with the NPA charges confirm the fact that beyond AgF_5^-, the AgF_n^- species exist as either (AgF_{n-2}^-)F_2 or F(AgF_{n-3}^-)F_2 complexes.

The distribution of the extra electronic charge as one moves from the neutral to anionic AgF_n clusters was analyzed by calculating the NPA charges. The charges on each atom of AgF_n are given in parentheses in Figures 2 and 3. In AgF, $-0.81e$ electron charge is transferred from Ag to F which is characteristic of an ionic bond. As successive F atoms are attached, this charge transfer from Ag increases rapidly but saturates at $+1.56e$ on Ag atom in AgF_3. In AgF^-, the extra electron is primarily located on the Ag site (See Figure 3). However, as size of the cluster increases, the extra-electronic charge is mostly delocalized over the F atoms. Note that the charge on the Ag atom in AgF_n^- is almost same as that in neutral AgF_n for $n > 3$ (See Figures 2 and 3). This is a characteristic of superhalogens and is the reason for the large electron affinity of AgF_n clusters as will be discussed below.

The electron affinity (EA) values of AgF_n are given in Table 2. The EA is defined as the energy difference between the ground states of the anion and its corresponding neutral and thus measures the energy gain in adding an electron to the neutral cluster. We see from Table 2 that the EA of AgF is rather small, namely 1.74 eV, but increases dramatically to 4.76 eV in AgF_2. Note that the electron affinity of Ag is 1.30 eV[21−23] and that of the F atom is 3.4 eV.[24] Thus, AgF_2 is already a superhalogen. The electron affinities continue to rise as successive F atoms are attached and reach a value of 7.11 eV in AgF_4. For AgF_n ($n = 5-7$), the EA values do not change significantly until one reaches AgF_7. The reason for such an anomalous behavior in the EA values beyond AgF_4 is because in the case of AgF_5, the neutral species is (AgF_3)F_2 complex, while the corresponding anion is (AgF_4^-)F complex. This composite structural feature is reflected in EA value of AgF_5, which is in fact, slightly smaller than the EA of AgF_4. Similarly, AgF_6, in both neutral and anionic cases, is in fact, (AgF_4)F_2

TABLE 2: Electron Affinities of XF_n (X = Cu, Ag, and Au; $n = 1-7$) clusters[a]

cluster	Cu	Ag	Au
XF	1.53	1.74	2.46
XF_2	3.79	4.76	4.84
XF_3	5.86	5.55	5.15
XF_4	6.91	7.11	6.85
XF_5	6.87	7.01	7.41
XF_6	7.03	7.24	8.38
XF_7	6.99	8.04	7.95

[a] All values are given in eV.

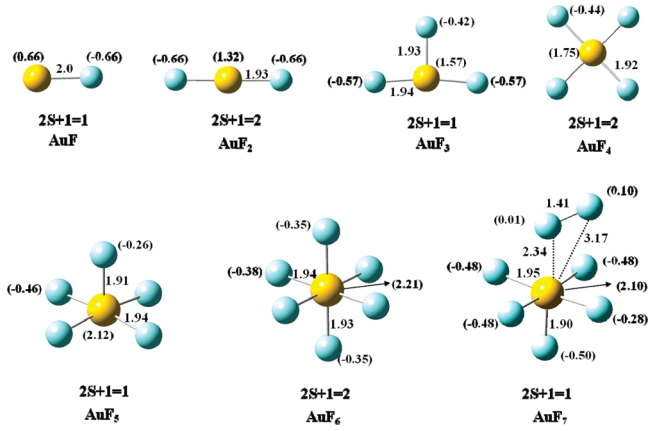

Figure 4. Equilibrium geometries of neutral AuF_n ($n = 1-7$) clusters along with their preferred spin multiplicities. The numbers in the parentheses are the NPA charges. All the bond lengths are given in Å.

complex. Therefore, it is the signature of AgF_4 cluster (7.11 eV) that is reflected in the EA value of AgF_6 (7.24 eV). In addition, as the cluster size increases, there are sudden spikes or jumps in the EA values of AgF_n clusters. For example, as one moves from AgF to AgF_2, the EA increases by 3.02 eV, while in the case of AgF_3 to AgF_4, the increase in the EA value is 1.56 eV. These large increments in the EA values reflect the enhanced stability of AgF_2^- and AgF_4^- over their immediate neighbors. The origin of the unusual stability of these anionic species is discussed below in the chemical bonding section (Section III). The fact that AgF_n ($n = 1-4$) clusters possess such large electron affinities indicates that stable salts can be synthesized by finding suitable counterions. As mentioned earlier, the highest oxidation state of Ag in a fluoride salt has been found to be +3. We hope that this work will stimulate experimentalists in the search of other salts where Ag can exist in oxidation states higher than that known thus far.

B. AuF_n Clusters. We now discuss our results for AuF_n clusters. Although both Ag and Au belong to the same group of coinage metals, their properties are very different. This is caused by relativistic effects in Au which are responsible for its many anomalous properties including that of its color. The equilibrium geometries of neutral and anionic AuF_n ($n = 1-7$) clusters are shown in Figures 4 and 5, respectively. The ground state spin multiplicities and the NPA charges (in parentheses) are also shown. Unlike in AgF_n clusters, the Au−F bond distances in the anions are larger than those in the neutrals. Similarly, the structures are also different. Here the F atoms bind dissociatively for all clusters up to $n = 6$, thus indicating that the oxidation state of Au can be as high as +6, when attached to F atoms. For AuF_7 cluster, two of the F atoms form a quasi-molecular structure and bind weakly to the Au atom while the remaining five F atoms bind atomically to the Au, thus forming $(AuF_5)F_2$ complex. The pentagonal bipyramidal structure, in which the Au atom can have an oxidation state of +7, even though a minimum on the potential energy surface, is about 2.09 eV higher in energy than the $(AuF_5)F_2$ complex. Our results for AuF_7 are in agreement with the recent work of Himmel et al.[14]

In Table 3 we list the dissociation/fragmentation energies of neutral and anionic AuF_n clusters analogous to those shown in eqs 1−5 except that here Ag is replaced by Au. We note that both the neutral and anionic AuF_n are stable against dissociation into AuF_{n-1} and F atoms over the entire size range. For the neutral cluster we further note that AuF_4 is more stable than

TABLE 3: Dissociation Energies of Neutral and Anionic AuF_n Clusters ($n = 1-7$)[a]

cluster	$\Delta E^{neutral}$	ΔE_n^{anion} (1)	ΔE_n^{anion} (2)	$\Delta \varepsilon_n^{neutral}$	$\Delta \varepsilon_n^{anion}$
AuF	2.65	2.89	1.63		
AuF_2	2.45	4.84	3.81	3.73	6.36
AuF_3	1.49	1.81	3.17	2.56	5.27
AuF_4	1.62	3.32	4.99	1.73	3.75
AuF_5	0.12	0.68	4.05	0.37	2.63
AuF_6	0.99	1.95	5.88	−0.27	1.27
AuF_7	0.70	0.26	5.16	0.31	0.83

[a] See eqs 1−5 for reference by replacing Ag with Au.

either AuF_3 or AuF_5 cluster. This is in contrast to the behavior of corresponding AgF_n clusters, where the stability against dissociation into AgF_{n-1} and F fragments decreased continuously from $n = 3$ to 5 (see Table 1). The most preferred dissociation pathway for anionic AuF_n^- ($n = 3-7$) clusters is found to be a neutral F atom and negatively charged AuF_{n-1}^- cluster, while in the fragmentation of AuF^- and AuF_2^- clusters, the negative charge is carried by the F atom. AuF_n^- clusters are also stable against fragmentation to AuF_{n-2}^- and F_2 molecule over the entire size range. However, in case of neutral species, AuF_6 is an exception. This is the only cluster that is unstable against fragmentation into AuF_4 and F_2. This anomalous result is due to the enhanced stability of AuF_4 cluster as discussed earlier. The instability of the AuF_6 cluster against dissociation into smaller species might hinder the Au to reach +6 oxidation state and one can conclude that the maximum oxidation state that Au can have while interacting with F atoms is +5. This conclusion is consistent with the earlier reported works[24,25] of Riedel et al.

The EA values of AuF_n clusters are given in Table 2. We note that the EA of AuF is 2.46 eV, which is larger than that of AgF. As successive F atoms are added, the electron affinities rise rapidly and reach a peak value of 8.38 eV for AuF_6. All the AuF_n clusters except AuF have electron affinities that exceed the value of Cl and hence can be classified as superhalogens. While no quantitative experimental value of the electron affinity of AuF_6 is available, it has been estimated[11] to be as high as 10 eV. That AuF_6^- is a well-known hexafluoride bears testimony to its large electron affinity. Our calculated EA of AuF_6 is in excellent agreement with a previously reported[13] value of 8.5 eV, obtained at CCSD(T) level. From Table 2, it is observed that there are certain sudden jumps in the EA values of AuF_n for $n = 2$, 4, and 6. For example, the EA increases by 2.38 eV as we move from AuF to AuF_2. On the other hand, the EA increases only marginally (0.31 eV) as we go from AuF_2 to AuF_3. Similar dramatic increases are observed at the cluster sizes of AuF_4 and AuF_6. These sudden increases in the EA values reflect the enhanced stability of AuF_2^-, AuF_4^-, and AuF_6^- clusters over their immediate neighbors. It is noteworthy here that in the case of AgF_n^- also we encountered unusually stable clusters at $n = 2$ and 4.

The large EA values of AuF_n clusters for $n > 1$ is due to the fact that the majority of the extra electronic charge is delocalized over the peripheral F atoms. This is evident by the NPA charges given in Figures 4 and 5. In the AuF anion, the extra electron redistributes over Au and F atoms, but most of it goes to the Au site that carries a positive charge. In large AuF_n^- clusters, the extra electron instead is distributed over the F atoms leaving Au in a positively charged state. Consequently the electron affinity increases and reaches a value as high as 8.4 eV. For example, as an electron is attached to the AuF_4 cluster, the extra electron is mostly delocalized over all the F atoms with only a

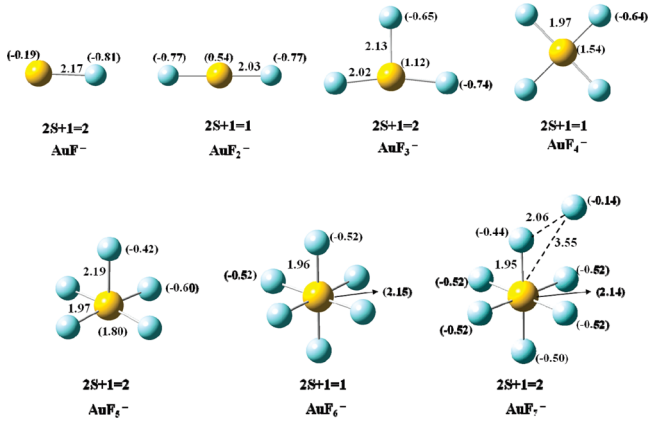

Figure 5. Equilibrium geometries of negatively charged AuF_n ($n = 1-7$) clusters along with their preferred spin multiplicities. The numbers in the parentheses are the NPA charges. All the bond lengths are given in Å.

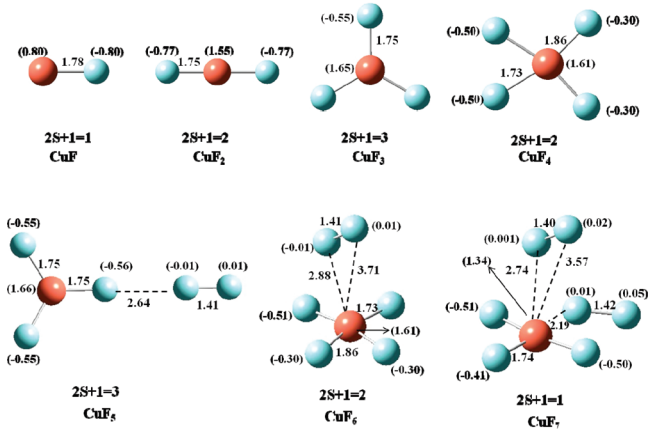

Figure 6. Equilibrium geometries of neutral CuF_n ($n = 1-7$) clusters along with their preferred spin multiplicities. The numbers in the parentheses are the NPA charges. All the bond lengths are given in Å.

partial charge of $-0.21e$ going to the Au atom. Similarly, if one compares the extra electron's charge distribution in AuF_5^- and AuF_6^-, we see that 30% of extra electron's charge is localized on Au in AuF_5^-, while in the case of AuF_6^-, Au atom gains only 6% of the extra electron's charge. Thus, in AuF_6^- the electron is more delocalized over F atoms than in AuF_5^-, which is manifested in the higher EA value of AuF_6^-. As more F atoms are attached transfer of charge from Au to F atoms increases and saturates at $+2.21e$ for AuF_6 cluster.

C. CuF_n Clusters. As mentioned earlier, to have a comparative study of all the coinage metal interactions with F on the same theoretical footing, we have calculated the equilibrium geometries of neutral and anionic CuF_n clusters. In Figures 6 and 7, we show the equilibrium geometries of CuF_n ($n = 1-7$) clusters corresponding to neutral and anionic states, respectively. Our results are in agreement with previous theoretical work[15] only up to the size of $n = 4$, where the F atoms are bonded to the central Cu atom dissociatively. However, when the number of F atoms is increased beyond 4, the F atoms start to form F_2 as is evident in the structures of neutral and anionic CuF_5 and CuF_6 (see Figures 6 and 7). Contrary to the reported highly symmetric structures[15] where all of the F atoms are bound to Cu dissociatively, we found lower energy structures for both neutral and anionic CuF_5 clusters where three F atoms bind dissociatively while two bind molecularly forming a $(CuF_3)F_2$ complex. In the case of neutral CuF_5, the previously reported

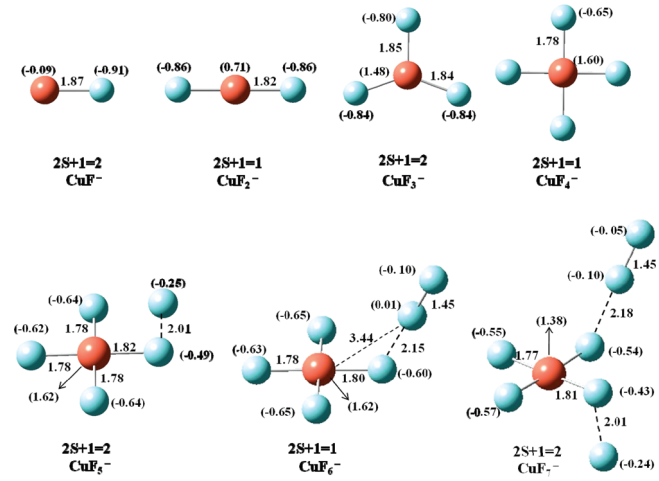

Figure 7. Equilibrium geometries of negatively charged CuF_n ($n = 1-7$) clusters along with their preferred spin multiplicities. The numbers in the parentheses are the NPA charges. All the bond lengths are given in Å.

square pyramidal structure (C_{4v}) was found to have imaginary frequencies. To find the corresponding structure that belongs to a minimum in the potential energy surface we moved the atoms of this C_{4v} isomer in the direction of the normal modes, corresponding to the imaginary frequencies and reoptimized the geometry. It resulted in a local minimum (C_s) structure, with the F atom moving away from the C_4 axis. This C_s structure was found to be 0.8 eV higher in energy than our reported $(CuF_3)F_2$ complex structure in Figure 6. It is to be noted here, however, that Wang et al.[15] used an all-electron basis set (cc-pVTZ-NR) for Cu, while in the current work, we have used the SDD basis set. To verify if the disagreement is due to different basis sets, we recalculated the geometry of Wang et al.[15] with the same all-electron basis set and found that the symmetric structure has imaginary frequencies, in agreement with SDD-based calculation. However, fixing the imaginary frequencies of the C_{4v} geometry did not result in the same C_s local minimum as obtained with the SDD-based calculation. On the other hand, the structure of CuF_5^- reported by Wang et al.[15] is in fact a local minimum but is 1.43 eV higher in energy than the geometry given in Figure 7. Although our computed geometries of both neutral and anionic CuF_5 clusters are different from those obtained by Wang et al.,[15] our computed electron affinity of 6.87 eV does not differ much from that obtained by Wang et al.,[15] namely 7.17 eV. In the case of CuF_6^-, the octahedron is found to be 1.06 eV higher in energy than our lowest energy isomer. Despite these disagreements, the conclusion of Wang et al.[15] that CuF_5 and CuF_6 are superhalogens remains unchanged. We also note that unlike their Ag and Au counterparts, CuF_3 and CuF_5 prefer triplet spin states (see Figure 6).

The dissociation energies of neutral and anionic CuF_n are given in Table 4. As expected, the most preferred dissociation channels and the stability of CuF_n follow a similar trend as the AgF_n clusters. In CuF_5 and CuF_6, the F_2 unit is barely bound to the CuF_3 and CuF_4 moieties, respectively. Similarly, one can conclude that CuF_6^- is actually $(CuF_4^-)F_2$ complex. The electron affinities of the CuF_n system are given in Table 2. The electron affinity is found to gradually increase with the increase in number of F atoms in the system as expected. However, similar to the trend observed in AgF_n clusters, the EA values remain approximately constant beyond CuF_4, again a strong signature of CuF_4 moiety in these larger species.

TABLE 4: Dissociation Energies of Neutral and Anionic CuF_n Clusters ($n = 1-7$)[a]

cluster	$\Delta E^{\text{neutral}}$	$\Delta E_n^{\text{anion}}(1)$	$\Delta E_n^{\text{anion}}(2)$	$\Delta \varepsilon_n^{\text{neutral}}$	$\Delta \varepsilon_n^{\text{anion}}$
CuF	3.88	4.10	1.92		
CuF_2	3.47	5.24	3.77	5.90	8.40
CuF_3	1.17	3.24	3.54	3.11	5.27
CuF_4	0.90	1.95	4.33	0.70	3.81
CuF_5	0.54	0.50	3.92	0.07	1.07
CuF_6	0.89	1.05	4.43	0.05	0.17
CuF_7	0.51	0.47	4.01	0.02	0.14

[a] See eqs 1−5 for reference by replacing Ag with Cu.

To summarize, we found that the structural properties exhibited by Cu are analogous to that of Ag, albeit with minor variations; Au maintains its unique character among the coinage metals by binding up to 6 F atoms dissociatively. Our results also indicate that the oxidation state of Cu in these systems can go only up to +4.

D. Chemical Bonding. In the earlier section, we have identified an important trend in the EA. Although the EA values continuously increase for all the coinage metals for each successive addition of F atom, as the charge is delocalized over several F atoms there are distinctive jumps at two, four, and six fluorine atoms. To understand the nature of bonding and explain the calculated trends in EA we have done natural bond orbital analysis on all of the systems presented. We focus on AuF_n systems because among the coinage metals gold forms the maximum Au−F bonds and also the EA are also much larger compared to others.

We begin our discussion with the diatomic AuF. Not surprisingly, the Au−F bond is highly polar; however, there is a significant amount of covalency involved in the bonding compared to either Cu−F or Ag−F. Addition of F^- alters the bonding considerably. NBO analysis identifies only one σ bond similar to the Au−F with significant Σ^* occupancy (0.222). The best way to describe the bonding in AuF_2^- is to consider an "ionic resonance" form in which F^- interacts with Au−F, as

$$F:^-Au-F \leftrightarrow F-Au^-:F$$

Formation of a resonance hybrid (a 3c−4e bond or ω-bond)[26−28] stabilizes the Au−F bond and the anion. This explains the sudden spike in the EA on going from AuF^- to AuF_2^-. In addition, the stabilization of the Au−F bond is also reflected in the dissociation energies as well, for example, dissociation of AuF_2^- to AuF + F^- (3.81 eV) is larger than Au−F bond energy (3.17 eV) in AuF_3^-. Next we consider AuF_4^- and AuF_6^-. Applying the same bonding scheme as described above, one can identify two and three 3c−4e bonds (or 2 and 3 ω-bonds), respectively. Note that the formation 3c−4e bonds require the participating atomic centers to be nearly linear. NBO analysis again identifies only two and three Au−F Σ bonds and large Σ^* occupancy. As in case of AuF_2^-, both a spike EA and large dissociation energies reflect the enhanced stability of AuF_4^- and AuF_6^-. Thus, the formation of one, two, and three 3c−4e bonds in AuF_2^-, AuF_4^-, and AuF_6^-, respectively, are responsible for their large EA values and extraordinary stabilities. Similar bonding features are also present in the corresponding Cu and Ag counterparts up to $n = 4$. However, the bonding in Au is more covalent as compared Cu and Ag. For example, comparison of electron localization function plots (Figure 8) of AuF_4^- and AgF_4^- clearly reflect the covalent character of Au−F bond.

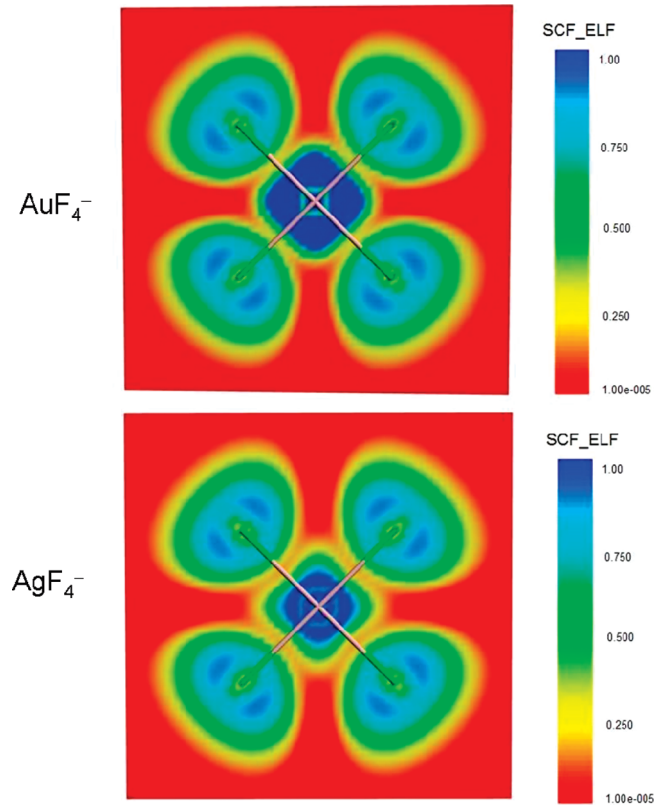

Figure 8. Iso-surfaces of electron localization plots of AuF_4^- and AgF_4^-.

IV. Conclusions

In summary, we have carried out a systematic study of the equilibrium geometries, electronic structure, relative stability, and electron affinity of XF_n (X = Cu, Ag, and Au; $n = 1-7$) clusters containing up to seven F atoms. Among the coinage metals, Au exhibits its uniqueness by forming stable clusters up to AuF_6. On the other hand, Cu and Ag can bind only up to 4 F atoms, dissociatively. In contrast to the earlier study, our current work shows that only four F atoms can be bound to Cu in atomic form, while the rest of the F atoms bind molecularly, resulting in either $[(CuF_3)F_2]$ or $[(CuF_4)F_2]$ complexes. We conclude that the maximum oxidation numbers/states of Cu and Ag are +4, while it is +6 for Au, when interacting with F atoms. Most importantly, the electron affinities of these clusters are very large reaching values as high as 8 eV. These values are larger than the electron affinity of Cl which has the highest value in the periodic table. The presence of 3c−4e (ω-bonds) in XF_n^- (X = Cu, Ag, and Au; $n = 2, 4$) and AuF_6^- are found to be responsible for their enhanced stabilities and high-electron affinities of their corresponding neutral clusters. Thus, XF_n anions can interact with alkali metal and other metal cations to give rise to very stable salts that contain a large amount of F atoms and hence are among the most powerful oxidizing agents. While no systematic experimental data on the electron affinity of coinage metal atoms interacting with halogens are available, we hope that the predictive capability of the theoretical method used here will motivate such experiments.

Acknowledgment. P.K. thanks Honors College of McNeese State University for providing partial financial support. P.K. and B.K. acknowledge partial support from Research Corporation. A.K.K. acknowledges Dr. Nikos for the faculty start-up funds made available through the Louisiana Board of Regents-

Research Commercialization/Educational Enhancement Program (RC/EEP). P.J. acknowledges partial support from the Defense Threat Reduction Agency and the Department of Energy.

References and Notes

(1) Knight, W. D.; Clemenger, K.; de Heer, W. A.; Saunders, W. A.; Chou, M. Y.; Cohen, M. L. *Phys. Rev. Lett.* **1984**, *52*, 2141.

(2) Bergeron, D. E.; Castleman, A. W., Jr.; Morisato, T.; Khanna, S. N. *Science* **2004**, *304*, 84.

(3) (a) Khanna, S. N.; Jena, P. *Phys. Rev. Lett.* **1992**, *69*, 1664. (b) Khanna, S. N.; Jena, P. *Phys. Rev. B* **1995**, *51*, 13705.

(4) Zheng, W.-J.; Thomas, O. C.; Lippa, T. P.; Xu, S.-J.; Bowen, K. H. *J. Chem. Phys.* **2006**, *124*, 144304.

(5) Gutsev, G. L.; Boldyrev, A. I. *Chem. Phys. Lett.* **1984**, *108*, 250.

(6) Gutsev, G. L.; Rao, B. K.; Jena, P.; Wang, X. B.; Wang, L. S. *Chem. Phys. Lett.* **1999**, *312*, 598.

(7) Gutsev, G. L.; Khanna, S. N.; Rao, B. K.; Jena, P. *Phys. Rev. A* **1999**, *59*, 3681.

(8) Scheller, M. K.; Compton, R. N.; Ceederbaum, L. S. *Science* **1995**, *270*, 1160.

(9) Compton, R. N.; Reinhardt, P. W. *J. Chem. Phys.* **1980**, *72*, 4655.

(10) (a) Graudejus, O.; Elder, S. H.; Lucier, G. M.; Shen, C.; Bartlett, N. *Inorg. Chem.* **1999**, *38*, 2503. (b) Lucier, G. M.; Shen, C.; Elder, S. H. *Inorg. Chem.* **1998**, *37*, 3829. (c) Riedel, S.; Kaupp, M. *Coord. Chem. Rev.* **2009**, *253*, 606.

(11) Compton, R. N. *J. Chem. Phys.* **1978**, *68*, 2023.

(12) Timakov, A. A.; Prusakov, V. N.; Drobyshevskii, Y. V. *Dokl. Akad. Nauk SSSR* **1986**, *291*, 125–128.

(13) Riedel, S.; Kaupp, M. *Inorg. Chem.* **2006**, *45*, 1228.

(14) Himmel, D.; Riedel, S. *Inorg. Chem.* **2007**, *46*, 5338.

(15) Wang, Q.; Sun, Q.; Jena, P. *J. Chem. Phys.* **2009**, *131*, 124301.

(16) Frisch, M. J.; Trucks, G. W.; Schlegel, H. B.; Scuseria, G. E.; Robb, M. A.; Cheeseman, J. R.; Montgomery, J. A., Jr.; Vreven, T.; Kudin, K. N.; Burant, J. C.; Millam, J. M.; Iyengar, S. S.; Tomasi, J.; Barone, V.; Mennucci, B.; Cossi, M.; Scalmani, G.; Rega, N.; Petersson, G. A.; Nakatsuji, H.; Hada, M.; Ehara, M.; Toyota, K.; Fukuda, R.; Hasegawa, J.; Ishida, M.; Nakajima, T.; Honda, Y.; Kitao, O.; Nakai, H.; Klene, M.; Li, X.; Knox, J. E.; Hratchian, H. P.; Cross, J. B.; Bakken, V.; Adamo, C.; Jaramillo, J.; Gomperts, R.; Stratmann, R. E.; Yazyev, O.; Austin, A. J.; Cammi, R.; Pomelli, C.; Ochterski, J. W.; Ayala, P. Y.; Morokuma, K.; Voth, G. A.; Salvador, P.; Dannenberg, J. J.; Zakrzewski, V. G.; Dapprich, S.; Daniels, A. D.; Strain, M. C.; Farkas, O.; Malick, D. K.; Rabuck, A. D.; Raghavachari, K.; Foresman, J. B.; Ortiz, J. V.; Cui, Q.; Baboul, A. G.; Clifford, S.; Cioslowski, J.; Stefanov, B. B.; Liu, G.; Liashenko, A.; Piskorz, P.; Komaromi, I.; Martin, R. L.; Fox, D. J.; Keith, T.; Al-Laham, M. A.; Peng, C. Y.; Nanayakkara, A.; Challacombe, M.; Gill, P. M. W.; Johnson, B.; Chen, W.; Wong, M. W.; Gonzalez, C.; Pople, J. A. *Gaussian 03*, Revision C.02; Gaussian, Inc.: Wallingford, CT, 2004.

(17) Becke, A. D. *J. Chem. Phys.* **1993**, *98*, 5648.

(18) Lee, C.; Yang, W.; Parr, R. G. *Phys. Rev. B* **1988**, *37*, 785.

(19) Kuznetsov, A. E.; Boldyrev, A. I.; Zhai, H.-J.; Li, X.; Wang, L.-S. *J. Am. Chem. Soc.* **2002**, *124*, 11791.

(20) Lucier, G. M.; Whalen, J. M.; Bartlett, N. *J. Flourine Chem.* **1972**, *89*, 101.

(21) Hotop, H.; Lineberger, W. C. *J. Phys. Chem. Ref. Data* **1985**, *14*, 731.

(22) Taylor, K. J.; Pettiettehall, C. L.; Cheshnovsky, O.; Smalley, R. E. *J. Chem. Phys.* **1992**, *96*, 3319.

(23) Bilodeau, R. C.; Scheer, M.; Haugen, H. K. *J. Phys. B* **1998**, *31*, 3885.

(24) Riedel, S.; Kaupp, M. *Angew. Chem., Int. Ed.* **2006**, *45*, 3708.

(25) Riedel, S.; Kaupp, M. *Inorg. Chem.* **2006**, *45*, 10497.

(26) Coulson, C. A. *J. Chem. Soc.* **1964**, 1442.

(27) (a) Pimentel, G. C. *J. Chem. Phys.* **1951**, *19*, 446. (b) Rundle, R. E. *Rec. Chem. Prog.* **1962**, *23*, 194.

(28) Weinhold, F.; Landis, C. R. *Valency and Bonding: A Natural Bond Orbital Donor-Acceptor Perspective*; Cambridge University Press: Cambridge, 2005.

JP101807S